Performance Analysis of Heterojunction with Intrinsic Thin Layer (HIT) Solar Cell

By

Shovon Talukder,

Abdus Sattar Prodhania, and

Kazi Peya Ahmed

Submitted to the

Department of Electrical and Electronic Engineering
Faculty of Sciences and Engineering
East West University

In partial fulfillment of the requirements for the degree of Bachelor of Science in Electrical and Electronic Engineering
(B.Sc. in EEE)

Summer, 2018

Approved by

Thesis Supervisor Dr. Anisul Haque Professor, Department of EEE East West University	Chairperson Dr. Mohammad Mojammel Al Hakim Professor, Department of EEE East West University

Abstract

Nanocrystalline Si:H (nc-Si:H) heterojunction with intrinsic thin layer (HIT) solar cells with the structure of ITO/nc-Si:H(P^+)/a-Si:H(i)/c-Si(n)/a-Si(i)/nc-Si:H(n^+)/Al is studied in this work. Photovoltaic properties of the solar cells such as, open circuit voltage, Short circuit current, fill factor and efficiency are investigated. We have selected emitter thickness, emitter concentration, work function of contact and absorber length to be varied, and the impacts of varying these on the basic solar cell parameters are presented. Standard AM1.5 spectrum for incident photon is used for this analysis. ATLAS SILVACO is used to construct and simulate the HIT Solar cell. The result shows that open circuit voltage, short circuit current, fill factor and overall efficiency are obviously affected by emitter concentration, emitter thickness and work function of the solar cell. The HIT solar cell gives the maximum current at a work function of 5.3eV of front contact. The emitter concentration at higher level gives a higher efficiency and an optimization in emitter thickness yield better cell efficiency as well. The absorber length doesn't affect the solar cell parameters.

Acknowledgement

This thesis is the result of determination and hard work done for twelve months. In the meantime, we are supported by many people. This is the time to express our gratitude to everyone.

At first, we want to thank our thesis supervisor Dr. Anisul Haque, Professor of Department of Electrical and Electronic Engineering of East West University for his affectionate guidance, innovative suggestion from the very beginning to the end of this task and supporting us with his profound knowledge through this study period on semiconductor materials. From the very beginning of this journey, his constructive suggestions helped us to learn about semiconductor materials and the basic properties of those. Without his support it was next to impossible for us to reach in the current stage with this thesis. We owe him lots of gratitude for guiding us with friendly behavior.

We further like to thank Dr. Mohammad Mojammel Al Hakim, professor and Chairperson of Department of Electrical and Electronic Engineering of East West University for supporting us with his profound knowledge in this study period. From the very beginning of this journey, his constructive suggestions helped us to learn ATLAS SILAVCO and basic properties of it. We further thank him for providing us with lab facilities.

Finally we want to thank our family for supporting us all the way this study, as well as thank to our entire friends and classmates for supporting us mentally

Authorization

We hereby declare that we are the sole author of this thesis. We authorize East West University to lend this thesis to other institutions or individuals for the purpose of scholarly research.

Shovon Talukder (SID: 2014-2-80-017)	Abdus Satttar Prodhania (SID: 2014-2-80-029)	Kazi Peya Ahmed (SID: 2014-2-80-020)

We further authorize East West University to reproduce this thesis by photocopy or other means, in total or in part, at the request of other institutions or individuals for the purpose of scholarly research.

Shovon Talukder (SID: 2014-2-80-017)	Abdus Satttar Prodhania (SID: 2014-2-80-029)	Kazi Peya Ahmed (SID: 2014-2-80-020)

Contents

Abstract.....2
Acknowledgement.....3
Authorization.....4
Contents.....5
List of Figures.....6
List of Tables.....8
Chapter 1: Introduction.....9
1.1 Literature Review.....9
1.2 Motivation.....10
1.3 Thesis Outline.....10
Chapter 2: Introduction to HIT solar cell.....11
2.1 Structure of HIT solar cell.....11
2.2 Key features of HIT solar cell.....14
Chapter 3: Simulation setup with SILVACO.....15
3.1 Model and Structure.....16
3.2 Comparison with the simulation of AMPS-1D.....19
Chapter 4: Results and Analysis.....22
4.1 J-V curve & Power curve analysis:.....22
4.2 Effect of the nc-Si:H (P^+) emitter thickness.....23
4.3 Effect of the doping concentration of the nc-Si: H (P^+) emitter.....25
4.3.1 Band bending trend due to concentration change of emitter.....27
4.4 Effect of the work function of the ITO layer.....29
4.4.1 Band bending trend due to work function change of ITO layer.....32
4.5 Effects of changing other parameters.....33
Chapter 5: Conclusion.....34
References:.....35

List of Figures

Figure 2.1: Hetero-junction (HIT) silicon solar cell. 12

Figure 2.2 (a): Energy band structure of the front side (nc-Si:H(p^+)/ a-Si:H(i)/c-Si(n)) of the HIT solar cell. 13

Figure 2.2 (b): Energy band structure of the back side (c-Si/a-Si:H(i)/ nc-Si:H(n^+)) of the HIT solar cell. 13

Figure 3.1: HIT solar cell structure (snap shot from TONYPLOT of ATLAS SILVACO). 15

Figure 3.1 (a): HIT solar cell structure (front side). 15

Figure 3.1 (b): HIT solar cell structure (back side). 16

Figure 3.2: J-V curve from AMPS-1D simulation result. 21

Figure 3.3: J-V curve from ATLAS SILVACO simulation result. 21

Figure 4.1: J-V curve of HIT solar cell. 22

Figure 4.2: Power curve of HIT solar cell. 22

Figure 4.3: The efficiency of HIT solar cell as a function of nc-Si:H p-layer thickness. . 23

Figure 4.4: The short circuit current of HIT solar cell as a function of nc-Si:H p-layer thickness. 24

Figure 4.5: The open circuit voltage of HIT solar cell as a function of nc-Si:H p-layer thickness. 24

Figure 4.6: The fill factor of HIT solar cell as a function of nc-Si:H p-layer thickness. . 25

Figure 4.7: The efficiency of HIT solar cell as a function of nc-Si:H p-layer concentration. 25

Figure 4.8: The short circuit current of HIT solar cell as a function of nc-Si:H p-layer concentration. 26

Figure 4.9: The open circuit voltage of HIT solar cell as a function of nc-Si:H p-layer concentration. 26

Figure 4.10: The fill factor of HIT solar cells as a function of the nc-Si:H (P^+) concentration. 27

Figure 4.11: Band bending of HIT solar cell as a function of nc-Si:H (P^+) concentration when $3\times10^{17}cm^{-3}$. 28

Figure 4.12: Band bending of HIT solar cell as a function of nc-Si:H (P^+) concentration when $3\times10^{18}cm^{-3}$. 28

Figure 4.13: Band bending of HIT solar cell as a function of nc-Si:H (P^+) concentration when $3\times10^{19}cm^{-3}$. 29

Figure 4.14: Work function of ITO effect on efficiency of HIT solar cell. 30

Figure 4.15: Work function of ITO effect on short circuit current of HIT solar cell.....30

Figure 4.16: Work function of ITO effect on open circuit voltage of HIT solar cell. 31

Figure 4.17: Work function of ITO effect on fill factor of HIT solar cell.....31

Figure 4.18: Band bending as a function of work function (4.8 eV) of ITO.....32

Figure 4.19: Band bending as a function of work function (5.0 eV) of ITO.....32

Figure 4.20: Band bending as a function of work function (5.3 eV) of ITO.....33

List of Tables

Table 3.1: Parameter set for the simulation of heterojunction solar cells with ATLAS SILVACO and AMPS-1D 20

Table 3.2: Comparison of the results between AMPS-1D and ATLAS SILVACO.....21

Table 4.1: Characteristics are remain unchanged due to the length of the c-Si absorber 33

Chapter 1: Introduction

Solar cells are electronic devices which directly convert sunlight into electricity. When solar radiation shines on a solar cell, it produces both current and voltage to generate electricity. For this process to occur, materials that can absorb light and generate electron-hole pairs are required. A good example is Silicon (Si). It is the most common type of semiconductor used in fabricating solar cells and other electronic devices. Currently in the market there exists three generations of solar cells used to harness the sun's energy. First generation has high conversion efficiency and has established industry. But first generation is made up of crystalline silicon and that needs a large amount of energy in fabrication than other two generations. It affects the environment and energy payback period. That is why 2^{nd} and 3^{rd} generation solar cell idea come in. The 2^{nd} generation is thin film technology. Less amount of inexpensive material and low efficiency are the characteristics of 2^{nd} generation. 2^{nd} generation initiated in 1980 and still this is running. CdTe (cadmium telluride), CIGS (copper-indium-gallium-diselenide), a-Si etc. are the examples of 2^{nd} generation. 3^{rd} generation is non-conventional solar cells. The primary target is to exceed Schokley-Queisser efficiency limit. Tandem solar cells are the example of 3^{rd} generation. High energy consumption during fabrication solved by low temperature fabrication process also solved out the issue of energy payback period and results in lower cost of solar energy.

In recent years, there have been many different solar cell designs and different materials are being studied to increase the efficiency of converting solar energy into electricity. The details of fabricating different types of solar cells are based on solid-state physics, chemistry, and material science. Nowadays, in the market there are mostly crystalline silicon technologies, thin- film technologies and other technologies (organic solar cells i.e. dye-synthesize solar cells). In early 90's, Sanyo, a Japanese company now owned by Panasonic fabricated a solar cell called "Hetero junction intrinsic thin layer solar cell" (HIT), which is a novel idea and will be explained in details in this thesis [1].

1.1 Literature Review

T. Sawada *et al.* [2] suggested in 1994 that a kind of Si heterojunction with intrinsic thin layer (HIT) solar cell gave 20% efficiency. The solar cell was based on n-type Czochralski Si textured absorber. The junction was fabricated at a low temperature of below 200° C. The stability under beam and low temperature fabrication process were emphasized on this report.

T. Mishima *et al.* [3] described in the paper that efficiency can be high with intrinsic thin layer solar cells at sanyo electric. They got conversion efficiency of 23.0% for a size of 100.4 cm^3 substrate. They found that HIT solar cell can be improved further in the cost performance scale.

Mikio Taguchi *et al.* [4, 5] suggested in their paper that, HIT solar cell has some striking features like better temperature co-efficient and higher open circuit voltage (V_{oc}). They had got 710 mV open circuit voltage by sticking to maintain a good interface throughout their fabrication process. They deal with open circuit voltage as an important basic parameter.

Congliang Zhang *et al.* [6] suggested a nanocrystalline Si:H (nc-Si:H) heterojunction with intrinsic thin layer (HIT) solar cell with the structure of ITO/nc-Si:H(p^+)/a-Si:H(i)/c-Si(n)/ a-Si:H(i)/nc-Si:H(n^+)/Al. They studied the photovoltaic properties of the cell. They studied by a numerical simulation software named AMPS-1D. The results show that an intrinsic a-Si:H

layer effectively reduces carrier recombination rate at interface. The simulated results also indicate that HIT solar cell with back surface field structure on n-type substrate can obtain higher performance.

T. Minami *et al.* [7] worked with the variation of work function of ITO layer. They showed how the work function of ITO layer can be changed and how it changes the efficiency. They found that the work function as well as the electrical, optical and chemical properties of transparent conducting multicomponent oxide films could be controlled by varying the chemical composition.

1.2 Motivation

Si nanocrystals embedded in hydrogenated amorphous silicon (a-Si:H) make nanocrystalline Si:H (nc-Si:H) film. It has high electrical conductivity, high mobility, high doping efficiency and low optical absorption as compared to hydrogenated amorphous silicon (a-Si:H) [8]. Mainly nc-Si:H has got many attentions now a days [9, 10], like better temperature co-efficient and high open circuit voltage. This is possible because the carrier recombination at heterojunction interface is reduced. The intrinsic thin amorphous silicon layer used in fabrication of present solar cells can be deposited by plasma enhanced chemical vapor deposition (PECVD) at low temperature like below 200°C and enables low energy consumption. When this process was done at above 800°C Si suffered a degradation. Hydrogenated amorphous silicon has instability too but nc-Si:H does not have any [11].

nc-Si:H has a promising chance to improve the efficiency level and become more stable [12].

nc-Si:H/c-Si heterojunction (HJ) has a large number of processing variables like, doping concentration of the nc-Si:H emitter, the thickness of the nc-Si:H emitter, the work function of the contact, the absorber thickness etc. that is why it is obvious that a leading change in the efficiency level can be made if the effect of each variable on the performance of HIT solar cell can be scrutinized experimentally. By doing simulation of solar cell numerically for precisely finding the role of various parameters using a combination of 2D and 3D device simulation program called ATLAS SILVACO will help us in a better way. We can get the desired results corresponding to our given inputs from this simulation more easily than from experiments.

1.3 Thesis Outline

This thesis report has five chapters. In chapter 1, introduction of photovoltaic technology as an alternative renewable energy is done and electronic characteristics of solar cell with short circuit current, open circuit voltage and efficiency are also discussed. Then the objective of this thesis is revealed along with the literature review and motivation part. In chapter 2, brief review of HIT solar cell with its structure and key features are discussed. In chapter 3, the code generated at ATLAS SILVACO for the simulation purpose are discussed step by step and made a comparison with AMPS-1D simulation result. In chapter 4, the result of this study is presented. The effect of changing different region values on solar cell parameters such as open circuit voltage, short circuit current, fill factor and efficiency are presented. Finally, the findings are concluded in chapter 5.

Chapter 2: Introduction to HIT solar cell

HIT solar cell means Heterojunction with Intrinsic Thin layer solar cell. In HIT Solar cell the nc-Si:H(p^+) will be the emitter and c-Si will be the absorber. HIT solar cells have numerous advantages i.e. possibility of higher efficiency than conventional solar cell, very good surface passivation which allows high open-circuit voltage. High open circuit voltage results in higher conversion efficiency which then require less area for mounting and number of modules to be installed are reduced. Thin intrinsic layers on and below the c-Si substrate effectively passivate c-Si surface defects, and help improve the junction characteristics. The major function of the intrinsic layer is to help reduce the recombination velocity of the holes and electrons in the doped a-Si: H material.

The design concept of HIT solar cell is very interesting and this chapter discusses the major design concept of this solar cell and compares it with other technologies. HIT solar cell is patented by Sanyo Electric Company in Japan, (now owned by Panasonic) and its currently popular among solar cell researchers, which has a conversion efficiency of 21.5% (open circuit voltage, V_{oc}: 0.712 V, short circuit current, I_{sc}: 3.837 A, fill factor, FF: 78.7%) with a practical size of 100.3 cm^2 [13].

2.1 Structure of HIT solar cell

We will now concentrate on the structure of a solar cell. A simple structure of solar cell consists of a transparent conductive oxide (ITO) on top, after that p-n junction of semiconductor material is used to separate the light excited charge carriers and a front metal contact and a back metal contact is used. When light falls on top, photons pass through the ITO layer since the band gap of the ITO material is very high than the energy of light photon. Then the photons energize the charge carriers; holes and electrons, which results in excess carrier generation in p-n regions, and the charge carriers diffuse through the depletion region. If the back contacts are connected to a load, charge carriers will flow through the load, and that is how we get electricity from a solar cell [14].

The schematic diagram of the HIT solar cells with a-Si:H (i) layers between p-type doped nc-Si:H emitter and c-Si (n) on the front side and between n-type doped nc-Si:H and c-Si (n) as a back surface field (BSF) structure on the back side is shown in figure 2.1.

The HIT solar cell is shown in figure 2.1. It consists of Six layers: ITO/nc-Si:H(p^+)/a-Si:H(i)/ c-Si(n)/a-Si:H(i)/nc-Si:H(n^+)/Al. Here the highly p-doped nc-Si:H and n-doped c-Si form a p^+/n diode. While the p-doped nc-Si:H, a-Si:H and n-doped c-Si form a p^+/i/n diode. Again, because the intrinsic amorphous layers are so thin, they do not contribute significantly to the electric field. A better way to increase the efficiency is to add a back surface field on the back side. A heavily doped nc-Si:H(n^+) layer is used as the back structure. The back surface field with highly doped n^+ creates a valence band offset and that can effectively reflect the minority carriers, holes here, to reduce the carrier recombination rate at the interface on the heterojunction. The conduction band offset makes a barrier for tunneling electrons which is the majority carriers, electrons here. A low concentration of majority carriers from c-Si(n)/nc-Si:H(n^+) interface is required to reduce the recombination rate there. So because of the back surface field a higher valence band offset and lower conduction band offset is made up and that enables better conversion efficiency of the cell.

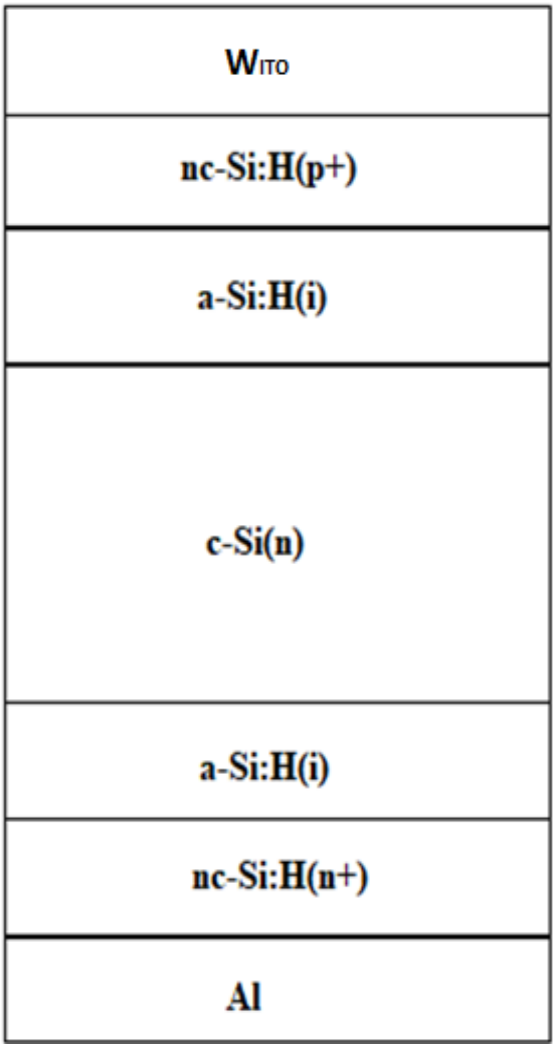

Figure 2.1: Hetero-junction (HIT) silicon solar cell.

Doped nc-Si:H film as p-type layer has lower absorption coefficient than that of a-Si:H in short-wavelength region so that more short-wavelength light will be absorbed in base area other than in p layer for better response. In addition doped nc-Si:H film better than doped a-Si:H because in nc-Si:H more dopant atoms can contribute to carriers which increases open circuit voltage. The doped nc-Si:H has high conductivity and reduces the series resistance of the emitter and results in high fill factor [6].

Here, energy band structure of HIT solar cell described in figure 2.1 is given in figure 2.2 (a) and figure 2.2 (b). The band gap of both nc-Si:H and a-Si:H is 1.8 eV. Only the absorber c-Si has band gap of 1.12 eV.

The band structure of HIT solar cell cannot be taken in a figure because the absorber length (c-Si) of the cell is comparatively very big than other regions. As a result, the band structure of HIT solar cell is shown by two segments. Figure 2.2 (a) and 2.2 (b) represents front side and back side of the cell respectively.

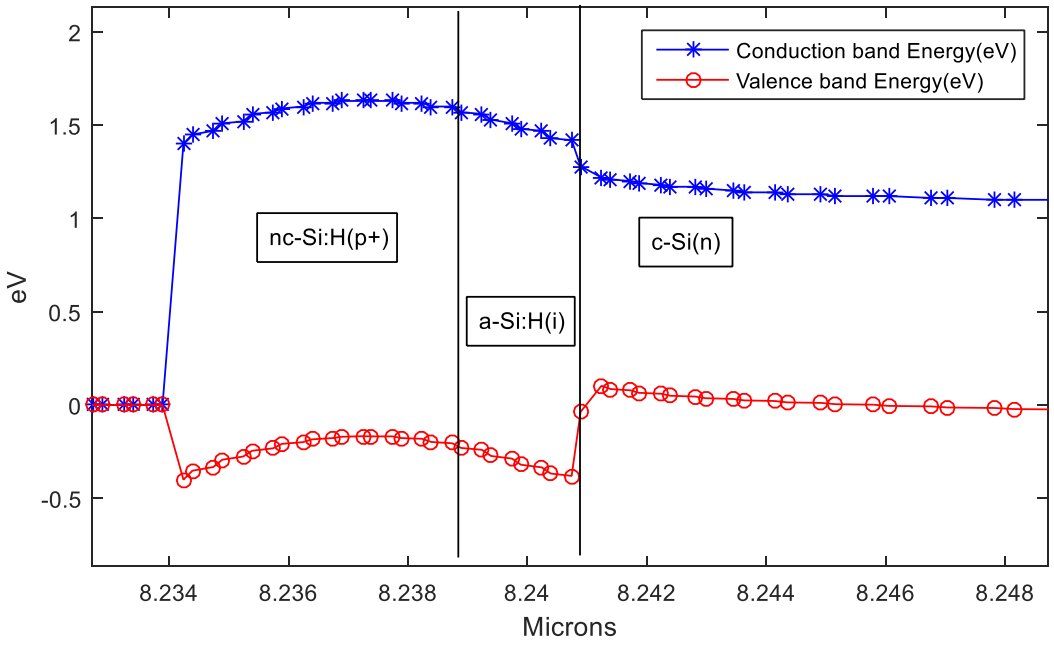

Figure 2.2 (a): Energy band structure of the front side (nc-Si:H(p^+)/ a-Si:H(i)/c-Si(n)) of the HIT solar cell.

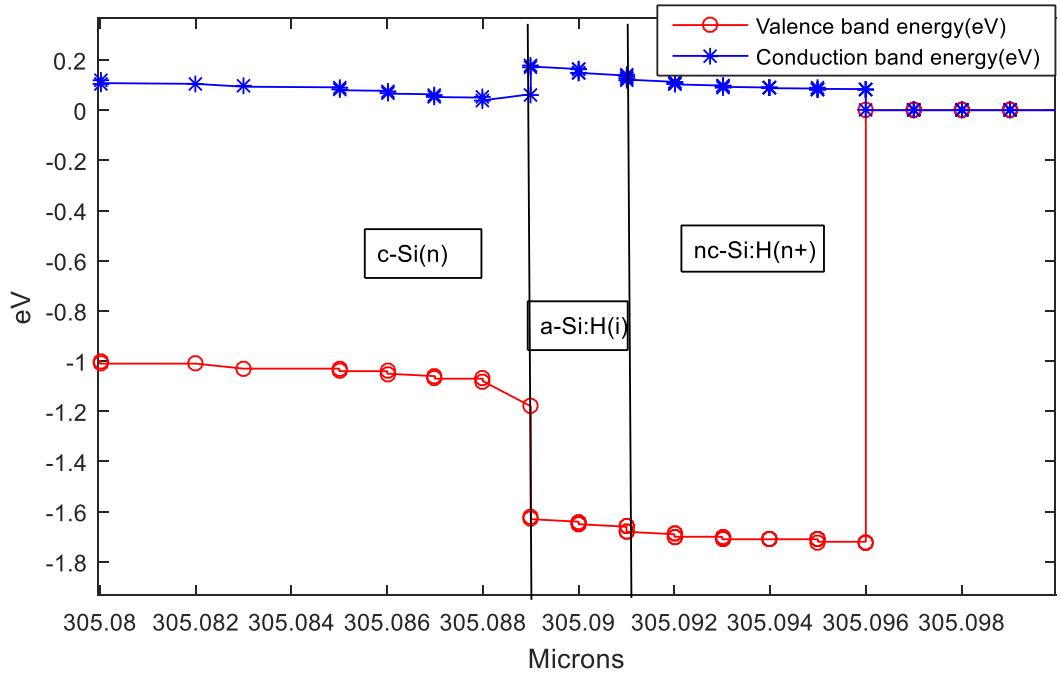

Figure 2.2 (b): Energy band structure of the back side (c-Si/a-Si:H(i)/ nc-Si:H(n^+)) of the HIT solar cell.

2.2 Key features of HIT solar cell

The three key features of HIT solar cells that give them an advantage based on performance over c-Si are reduction of optical and recombination losses and minimizing electric losses [13].

1. The recombination losses in the c-Si and at interface which could lead to losses of charge carries (recombination) and eventually reducing the performance of the cell have been corrected using an intrinsic amorphous silicon, which passivate the surface of the c-Si, disallowing charge carriers from escaping and also the improved structure of the a-Si:H reduces the recombination losses.

2. The optical losses at front and back contact, also at the ITO are being corrected by using low optical absorption material. This is done so as to increase the short circuit current of the cell. By using low absorption materials, the sun radiation goes straight into the absorber for power generation.

3. The electrode at the front grid of the HIT solar cell was reduced in thickness so as to minimize the shading effect and resistive losses. The resistive losses at the grid were corrected using low resistive silver. Further research is being carried out in order to improve the performance of HIT cells and also the cost reduction is being considered.

Chapter 3: Simulation setup with SILVACO

In this thesis, ATLAS SILVACO is used to simulate a solar cell structure having nc-Si:H(p^+) as p-type material, c-Si(n) as n-type material, an a-Si:H(i) as surface interface of n type and p type material, two contacts and a back surface field which consists of nc-Si:H(n^+) and a a-Si:H(i). The simulation of the HIT solar cell structure described in figure 2.1 is given in figure 3.1, 3.1 (a) and 3.1(b).

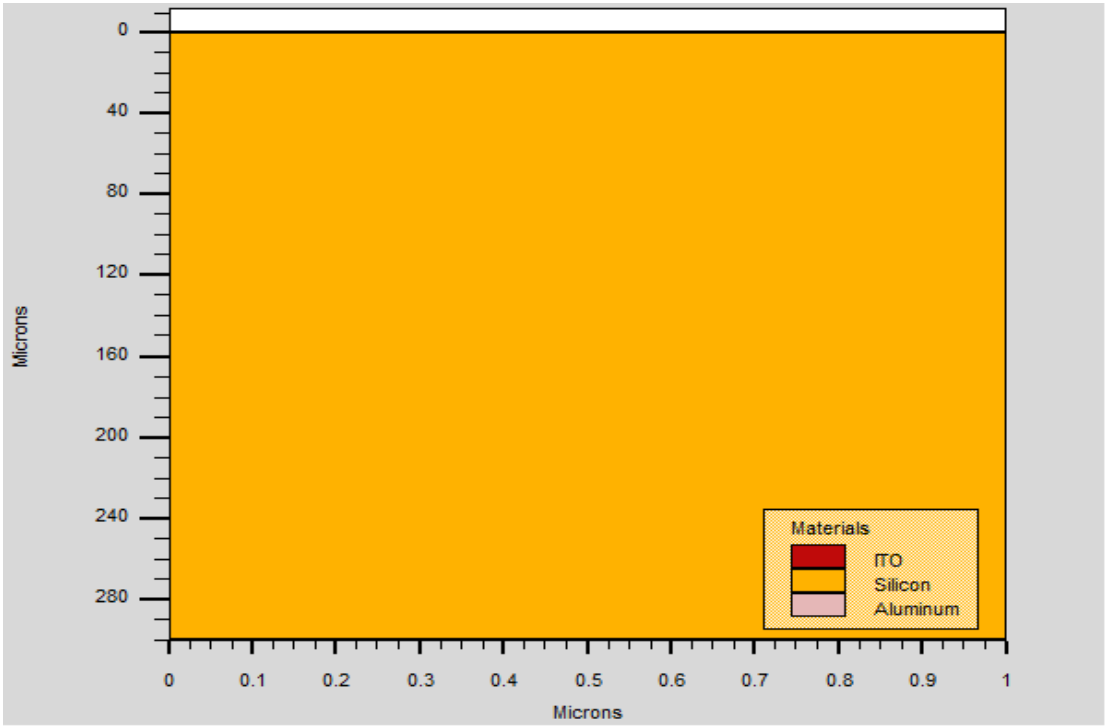

Figure 3.1: HIT solar cell structure (snap shot from TONYPLOT of ATLAS SILVACO).

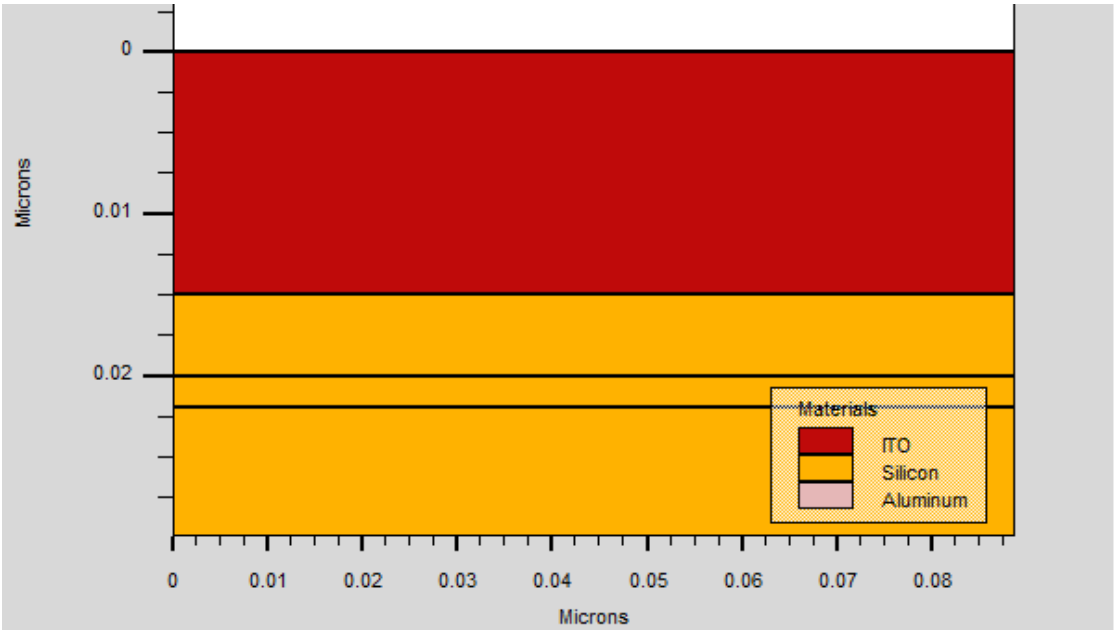

Figure 3.1 (a): HIT solar cell structure (front side).

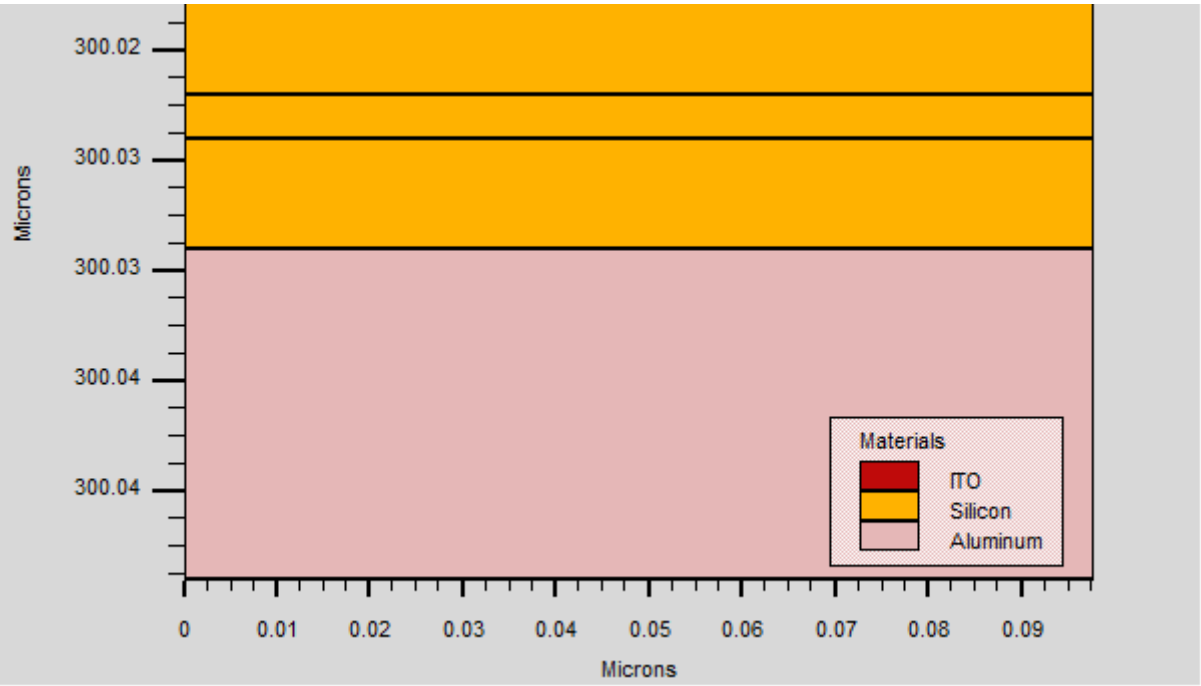

Figure 3.1 (b): HIT solar cell structure (back side).

Here, the overall structure is shown in figure 3.1. As the absorber region is too big than other regions, so front side and back side of the HIT solar cell are shown in 3.1 (a) and 3.1 (b) respectively.

3.1 Model and Structure

Here, the HIT Solar cell is simulated in ATLAS SILVACO through a text input run time environment, called DECKBUILD. Different cell parameters are studied from its manual and then the examples are followed strictly to implement all.

Some data values are implemented in the Simulation. They are discussed briefly.

Mesh:

Mesh is the specification of grid which divides the device in some horizontal and vertical lines. Mesh grid parameter affects the simulation process of the structure. In the simulation we have used x.mesh from 0.00 to 1.0 where spacing is 0.1, whereas we have used y.mesh from 0.00 to 300.044 where spacing is 0.0005.

Region:

Region defines the area of the device. By defining region, one can get the idea of the device area and range. In region, the used material is also defined. The material property only effective to the defined region independently. In this simulation x axis is same for all the regions. In the y-axis the regions are individually declared. ITO is from 0.00 to 0.015 in the y-axis, nc-Si:H (p^+) is from 0.015 to 0.02 in the y-axis, a-Si is from 0.02 to 0.022 in the y-axis, c-Si is from 0.022 to 300.022 in the y-axis. a-Si:H is from 300.022 to 300.024 in the y-axis. nc-Si:H (n^+) is from 300.02 to 0.022 in the y-axis, Aluminum is from 300.022 to 300.024 in the y-axis.

Electrode:

This part is used to specify and name the electrodes in the mesh and region part which is defined before. In the y-axis from 0.00 to 0.015 anode is declared whereas in the y-axis from 300.029 to 300.044 cathode is declared.

Doping:

The specification of the doping concentration of the materials is done using "doping" Statement. For example:

doping x.min = 0.0 x.max = 1.0 y.min =0.015 y.max = 0.02 p.type conc= 3*1e19 uniform
doping x.min = 0.0 x.max = 1.0 y.min =0.022 y.max = 300.022 n.type conc= 3*1e15 uniform

In the region y-axis from 0.015 to 0.02, the material is uniformly highly p type doped having user defined concentration in a predefined mesh. And also in the region y-axis from 0.022 to 300.022, the material is uniformly n type doped having user defined concentration in a predefined mesh.

Material:

Using "material", different properties and physical parameters of previously defined and doped regions are selected from the ATLAS database. For example:

Material region=2 taun0=1e-6 taup0=1e-6 affinity=3.9 eg300=1.8 nv300=2.5e20 nc300=2.5e20 eab=0.03 edb=0.06
Mobility region=2 mun300=200 mup300=20

Here, in the region 2 which is nc-Si:H(P^+), electron and hole Shockley-Read-Hall recombination lifetimes is 1e-6. Electric affinity is 3.9 eV, Band gap at 300k is 1.8 eV. The valence band effective density-of-states at 300 K is 2.5e20 cm^{-3} and conduction band effective density-of-states at 300 K is 2.5e20 cm^{-3}. The acceptor energy level is 0.03 and donor energy level is 0.06. Low field electron mobility is 200 cm^2/Vs, low field hole mobility is 20 cm^2/Vs.

INTDEFECTS region=2 EGA=0.7 EGD=1.22 SIGGAE=1e-15 SIGGAH=1e-17 SIGGDE=1e-17 SIGGDH=1e-15

INTDEFECTS activates the band gap interface defect model and sets the parameter values. Here, EGA=0.7eV specifies the energy that corresponds to the Gaussian distribution peak for acceptor-like states. This energy is measured from the conduction band edge. EGD=1.22eV Specifies the energy that corresponds to the Gaussian distribution peak for donor-like states. This energy is measured from the valence band edge. SIGGAE specifies the capture cross-section for electrons in a Gaussian distribution of acceptor-like states. SIGGAH Specifies the capture cross-section for holes in a Gaussian distribution of acceptor-like states. SIGGDE specifies the capture cross-section for electrons in a Gaussian distribution of donor-like states. SIGGDH Specifies the capture cross-section for holes in a Gaussian distribution of donor like states.

Defects:

The a-Si intrinsic layer must have defects layer. These are taken from manual and example of ATLAS SILVACO a-Si simulation declaration part.

defect region=3 cont nta=2e20 ntd=2e20 wta=0.028 wtd=0.055 \
nga=0 ngd=0 ega=1.22 egd=1.22 wga=0.188 wgd=0.188 \
numa=50 numd=50 sigtae=1.e-16 sigtah=1.e-16 sigtde=1.e-16 sigtdh=1.e-16

defects region=3 amphoteric cont signp=1e-14 sign0=5e-15 sigp0=5e-15 sigpn=1e-14 \
hconc=2e21 nsisi=2e23 sigma=0.19 t0=500 ev0=0.045 eu=0.2 \
ep.amp=1.22 num.amp=50 nv0.amp=1e20

Model:

Using "model" statement, specified and required physical model is declared for simulating the structure. The physical models are divided into five classes: mobility, recombination, carrier statistics, impact ionization, and tunneling.

models srh temperature=300

In this thesis, Shockley-Read-Hall (SRH) recombination model was used. The theory of photon transition in the presence of defect within the forbidden gap of the semiconductor was first derived by Shockley and Read and then by Hall. The SRH recombination is modeled as equation 3.1.

$$R_{SRH}=\frac{pn-n_{ie}^2}{TAUP0\left[n+n_{ie}\exp\left(\frac{ETRAP}{KT_L}\right)\right]+TAUN0\left[p+n_{ie}\exp\left(\frac{-ETRAP}{KT_L}\right)\right]} \quad \ldots\ldots 3.1$$

Here, ETRAP is the difference between the trap energy level and the intrinsic Fermi level, TL is the lattice parameter in degree kelvin, and TAUN0 and TAUP0 are the electron and hole lifetimes. Using "SRH" parameter of the model statement, this recombination model is declared.

Reflection:

In the cathode and anode the reflection is to be set up. For example,

Contact name = anode reflect=0.1 SURF.REC VSURFN=1e6 VSURFP=1e6
Contact name = cathode reflect=1 SURF.REC VSURFN=1e6 VSURFP=1e6

Here, the light reflection of the front and the back contacts was set to be 0.1 and 1, respectively. The surface recombination velocities of both electrons and holes were set as 1×106 cm/s.

Beam:

Using "beam" statement, optical beam is declared. For example:

beam num=1 angle=90 am1.5 wavel.start=0.300 wavel.end=1.1 wavel.num=100

Here, one beam is defined, and the AM1.5 spectrum is used and the range of wavelength is also defined to simulate the solar cell defined earlier.

Log:
Using this statement, a log file is opened. A particular name of the log file should be given.

LOG OUTFILE="HIT.LOG"

Here, a log file whose name is" HIT.LOG" is declared to store the simulated results.
Solve:
This statement follows a statement and further a solution is performed for some user defined bias points.

SOLVE VANODE=0 NAME=ANODE VSTEP=0.01 VFINAL=0.8

Here, the simulation is performed for anode voltage range. The difference between each bias point is 0.01 Vs. The results are saved in the log file declared earlier.

Tonyplot:
This command is used to see the plot of log file and structure file. Structure file saves the structure of the cell defined earlier. For example:

TONYPLOT HIT.LOG

Here, this statement is used to see the plot of the desired log file.

3.2 Comparison with the simulation of AMPS-1D

There are some reasons for not choosing AMPS-1D. One can easily see the every step simulation result in ATLAS SILVACO. ATLAS SILVACO enables the characterization and optimization of semiconductor devices for a wide range of technologies. Device simulation helps users understand and depict the physical processes in a device and to make reliable predictions of the behavior of the next device generation. Two-dimensional device simulations with properly selected calibrated models and a very well-defined appropriate mesh structure are very useful for predictive parametric analysis of novel device structures. Two- and three-dimensional modeling and simulation processes help users obtain a better understanding of the properties and behavior of new and current devices. This helps provide improved reliability and scalability, while also helping to increase development speed and reduce risks and uncertainties. On the other hand AMPS-1D simulation is one dimensional. It uses few basic equations which does not allow to manipulate many phenomena. Different type of defects cannot be included in the simulation, such as anti-site, vacancy, mismatch, interface etc. It results in only ideal cases under standard condition most of the times. It has discrete grid points instead of being continuous. During practical fabrication process, loss mechanism or generation- recombination happen which is not possible to include in AMPS-1D.
For the simulation of HIT solar cell in both ATLAS SILVACO and AMPS-1D, an initial set of parameters for all the properties of the nanocrystalline, amorphous and crystalline silicon materials were needed and the values were listed in Table 3.1. The operation temperature was set at 300 K, the AM1.5 source was adopted as the solar radiation with a power density of 100

mW/cm^2, and the effective wavelength range was 300 nm-1100 nm, the corresponding absorption coefficient is obtained from [15]. The light reflection of the front and the back contacts was set to be 0.1 and 1, respectively. The surface recombination velocities of both electrons and holes were set as 1×10^6 cm/s [16].

Using Table 3.1 the simulations are done in both ATLAS SILVACO and AMPS-1D software. Here, figure 3.2 represents the J-V curve, simulated in AMPS-1D. The structure of figure 2.1 is followed and the simulation is done using parameters of table 3.1. The figure shows the J-V curve with the values of short circuit current density, efficiency, fill factor and open circuit voltage.
Figure 3.3 represents the J-V curve, simulated in ATLAS SILVACO. The structure of figure 2.1 and material properties of table 3.1 are also followed in this simulation.

Table 3.1: Parameter set for the simulation of heterojunction solar cells with ATLAS SILVACO and AMPS-1D

Parameter e, h for electrons and holes, respectively	**nc-Si:H(p+)**	**a-Si:H(i)**	**nc-Si:H(n+)**	**c-Si(n)**
Thickness (nm)	5	2	5	300,000
Electron affinity (eV)	3.9	3.9	3.9	4.05
Bandgap (eV)	1.8	1.8	1.8	1.12
Effective conduction band density(cm^{-3})	2.5×10^{20}	2.5×10^{20}	2.5×10^{20}	2.8×10^{20}
Effective valence band density (cm^{-3})	2.5×10^{20}	2.5×10^{20}	2.5×10^{20}	1.04×10^{20}
Electron mobility ($cm^2\ V^{-1}\ s^{-1}$)	200	20	200	1350
Hole mobility ($cm^2\ V^{-1}\ s^{-1}$)	20	2	20	450
Acceptor concentration (cm^{-3})	3×10^{19}	0	0	0
Donor concentration (cm^{-3})	0	0	1×10^{19}	3×10^{15}
Characteristic energy (eV) for donors, acceptors	0.06,0.03	0.06,0.03	0.06,0.03	0.01,0.01
Gaussian peak energy (eV) donors, acceptors	1.22, 0.7	1.22, 0.7	1.22, 0.7	
Capture cross-section for donor states, e, h (cm^2)	1×10^{-17}, 1×10^{-15}	1×10^{-17}, 1×10^{-15}	1×10^{-17}, 1×10^{-15}	1×10^{-17}, 1×10^{-15}
Capture cross-section for acceptor states, e, h (cm^2)	1×10^{-15}, 1×10^{-17}	1×10^{-15}, 1×10^{-17}	1×10^{-15}, 1×10^{-17}	1×10^{-15}, 1×10^{-17}

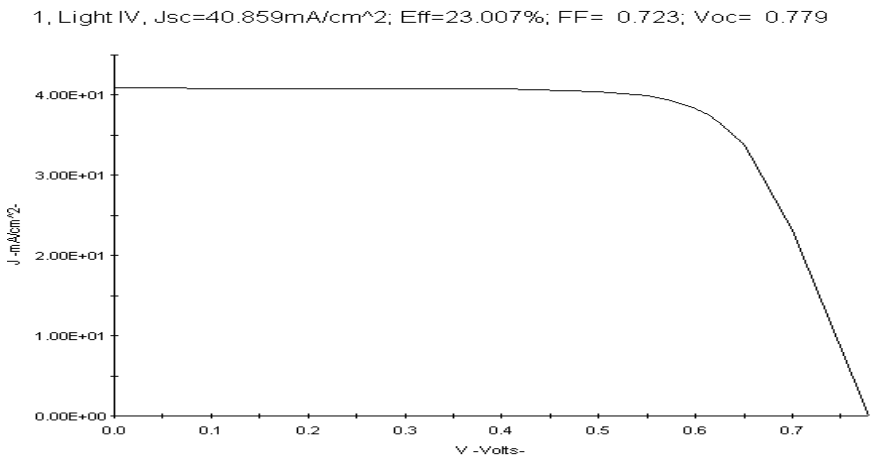

Figure 3.2: J-V curve from AMPS-1D simulation result.

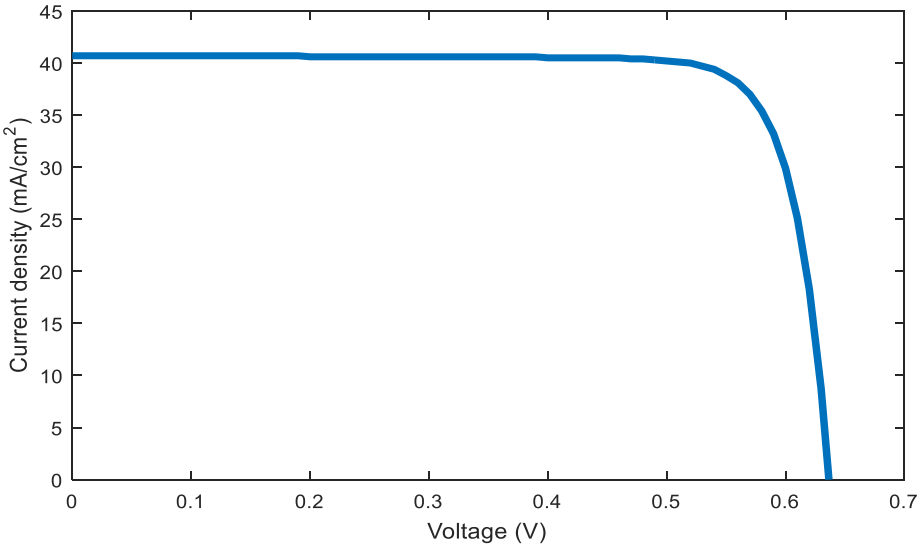

Figure 3.3: J-V curve from ATLAS SILVACO simulation result.

Table 3.2: Comparison of the results between AMPS-1D and ATLAS SILVACO

Simulation software	Short circuit current density (mA/cm^2)	Open circuit voltage (V)	Fill factor (%)	Efficiency (%)
ATLAS SILVACO	40.72	0.636	82.44	21.37
AMPS-1D	40.85	0.779	72.3	23.007

From table 3.2, it is observed that both the simulation software gave almost same current. But AMPS-1D gave higher open circuit voltage whereas ATLAS SILVACO gave higher fill factor. AMPS-1D gave higher efficiency than ATLAS SILVACO simulation software.
Although AMPS-1D gave higher efficiency, we mainly used ATLAS SILVACO simulation software for better understanding the physics.

Chapter 4: Results and Analysis

The results are obtained from ATLAS SILVACO simulation. Simulated results are extracted through Microsoft Excel and plotted in MATLAB. We simulated the device structure shown in figure 2.1. The parameter values are taken from table 3.1.

4.1 J-V curve & Power curve analysis:

Here, J-V curve represents the anode current density versus anode voltage of the solar cell. The heterojunction intrinsic thin solar cell provides short circuit current of 40.86 mA/cm^2 and open circuit voltage of 0.63V. Figure 4.1 shows the J-V characteristics.

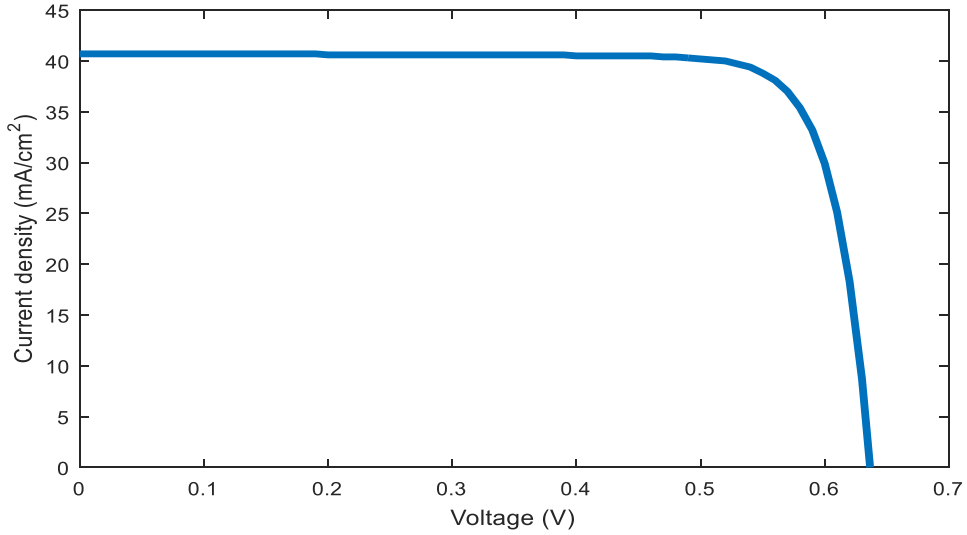

Figure 4.1: J-V curve of HIT solar cell.

The power curve simulated using the proposed model has been shown in figure 4.2. It is noteworthy that the maximum power is 21.37 mW/cm^2 obtained in the proposed model. At maximum power, the maximum voltage is 0.55 V and maximum current is 38.84 mA/cm^2.

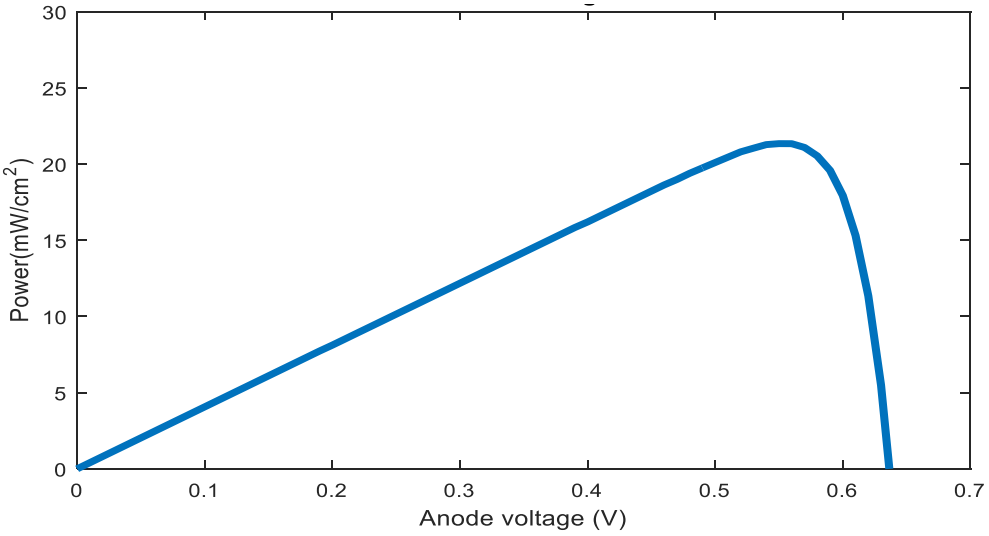

Figure 4.2: Power curve of HIT solar cell.

4.2 Effect of the nc-Si:H (P^+) emitter thickness

If the emitter is too thin, it will completely become depleted and cannot form a p-n junction. So with the increase of the emitter thickness, at first the solar cell efficiency will increase and then decrease gradually. It is clear that with increasing the thickness of the emitter, built-in potential increases slowly so that makes open circuit voltage increase negligibly as shown in figure 4.5. The efficiency increases slightly because of the built-in potential too. On the other hand, the series resistance increases with the increase of the emitter thickness, which leads to the decline of the efficiency and fill factor (FF), as shown in figure 4.3 and figure 4.6, which is negligible too. A solar cell with efficiency of 21.37% is obtained at the optimum emitter thicknesses of 5nm [6]. But the change is negligible to consider and it is shown in figure 4.3. If the emitter is too thick the short-wavelength response gradually worsens and thus the short-circuit current is decreased slowly as described in figure 4.4, which is also negligible. But if the emitter is too thin, it will completely become depleted and cannot form a p-n junction.
The changes of the thickness of the emitter and thus the result of it on characteristics of the HIT solar cell are shown from figure 4.3 to 4.6. Results in figure 4.3 to 4.6 clearly show that performance of solar cell for all practical purpose does not depend on emitter thickness. Here, the rest of the parameters of the HIT solar cell remain unchanged as followed the table 3.1.

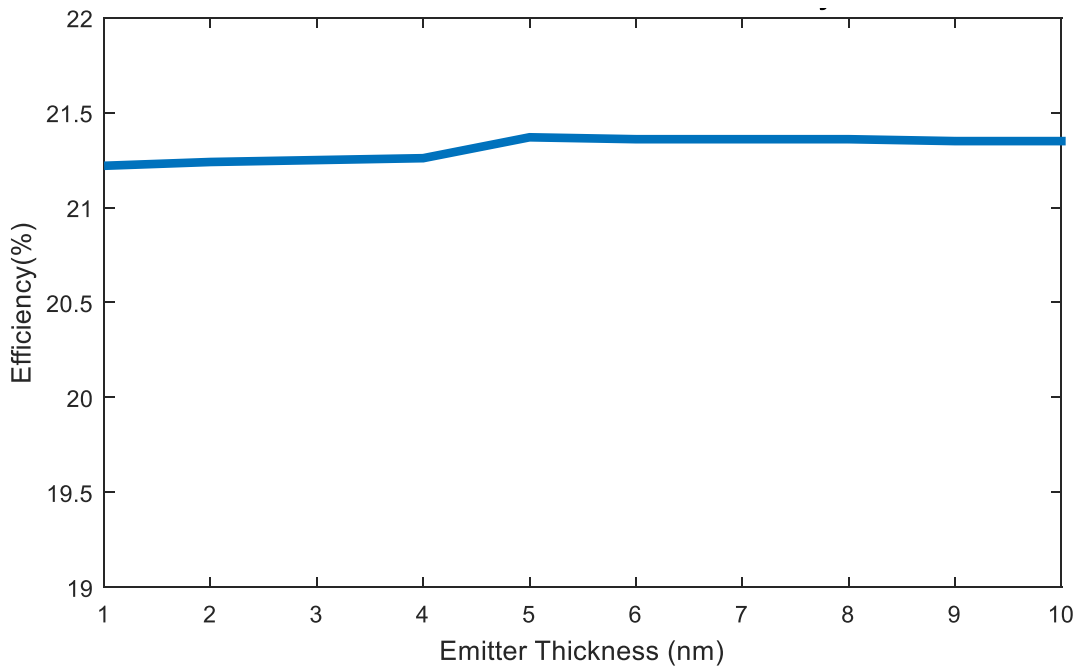

Figure 4.3: The efficiency of HIT solar cell as a function of nc-Si:H p-layer thickness.

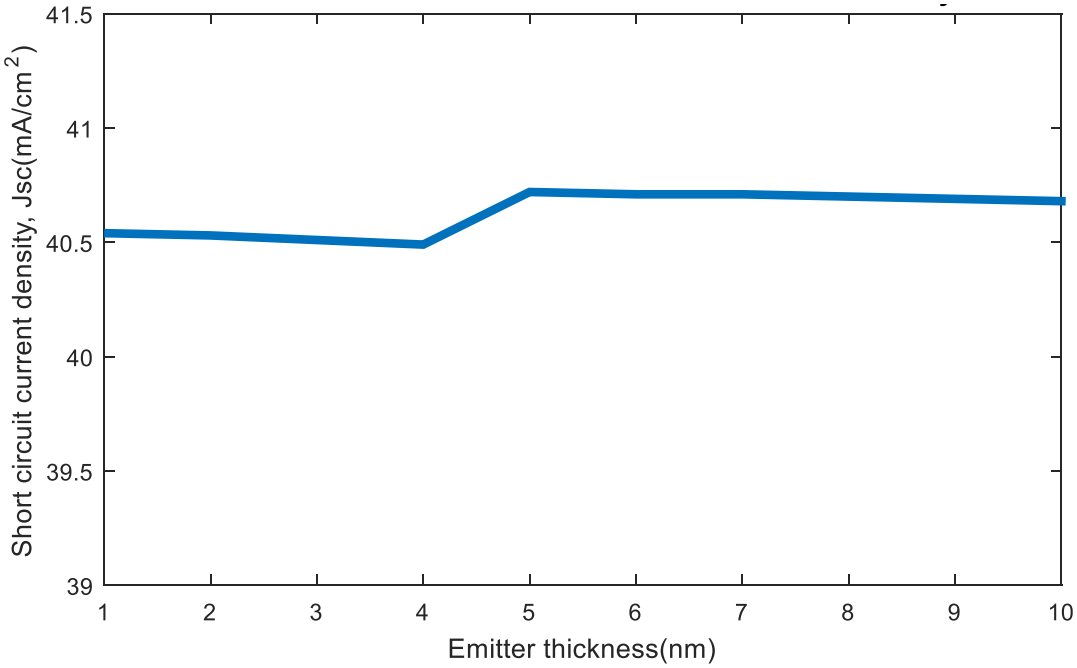

Figure 4.4: The short circuit current of HIT solar cell as a function of nc-Si:H p-layer thickness.

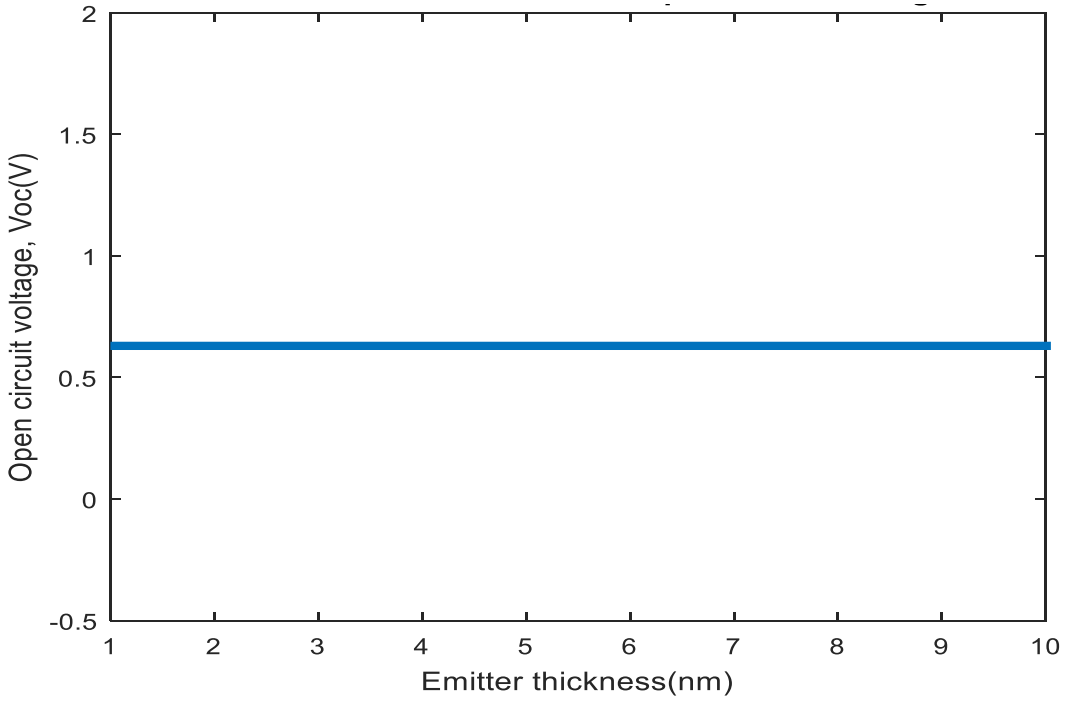

Figure 4.5: The open circuit voltage of HIT solar cell as a function of nc-Si:H p-layer thickness.

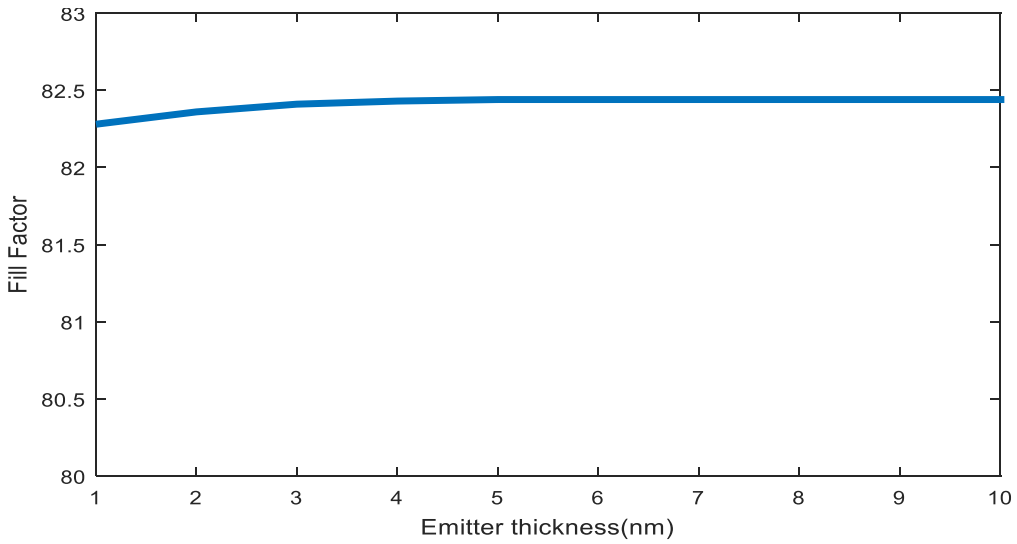

Figure 4.6: The fill factor of HIT solar cell as a function of nc-Si:H p-layer thickness.

4.3 Effect of the doping concentration of the nc-Si: H (P^+) emitter

We observe that if we increase the emitter concentration from 3×10^{17} cm^{-3} to 3×10^{18} cm^{-3} then the current, voltage and efficiency slightly increased. But we get a huge increase in efficiency when the concentration changed to 3×10^{19} cm^{-3} shown in figure 4.7. The current remain unchanged but efficiency changes due to voltage rise. A very high doping concentration is unacceptable because of the inferior optoelectronic properties of the heavy doped nc-Si:H emitter. In addition to this, a large doping concentration than 3×10^{19} cm^{-3} is difficult to obtain in the laboratory [6, 15].

The changes of the doping concentration of the emitter and thus the results of it on characteristics of the HIT Solar cell are shown from figure 4.7 to 4.10. Here, the rest of the parameters of the HIT solar cell remain unchanged as followed the table 3.1.

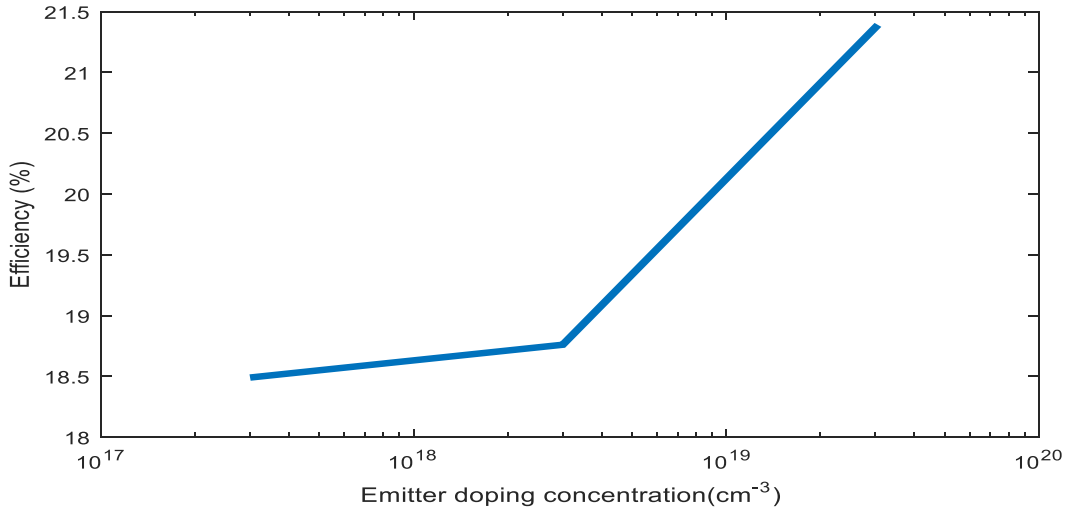

Figure 4.7: The efficiency of HIT solar cell as a function of nc-Si:H p-layer concentration.

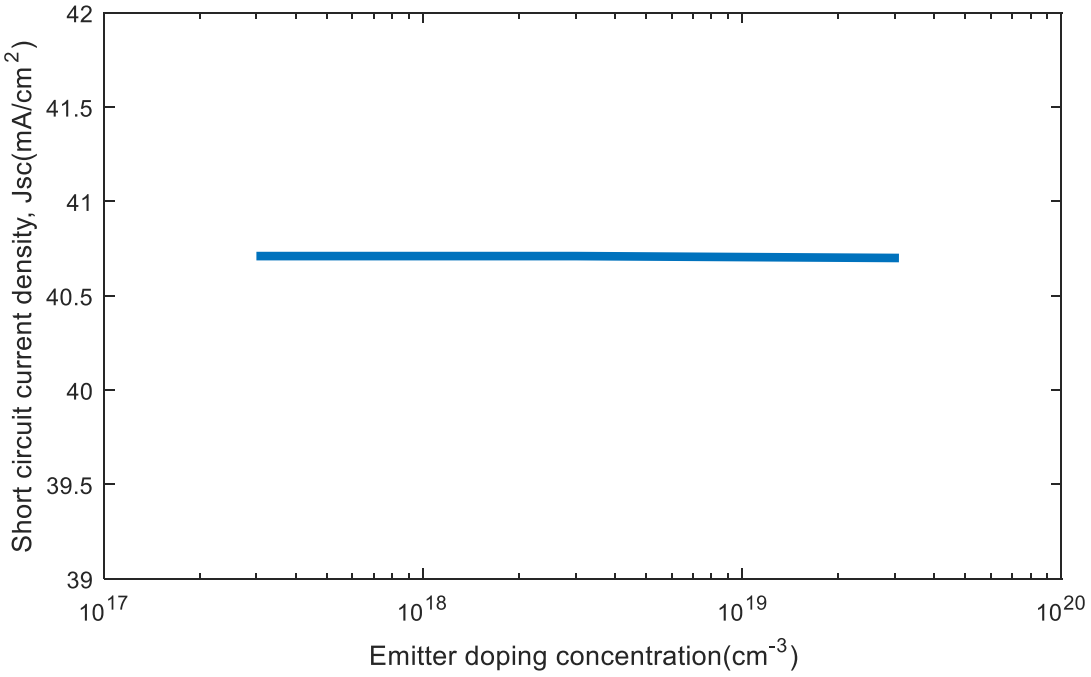

Figure 4.8: The short circuit current of HIT solar cell as a function of nc-Si:H p-layer concentration.

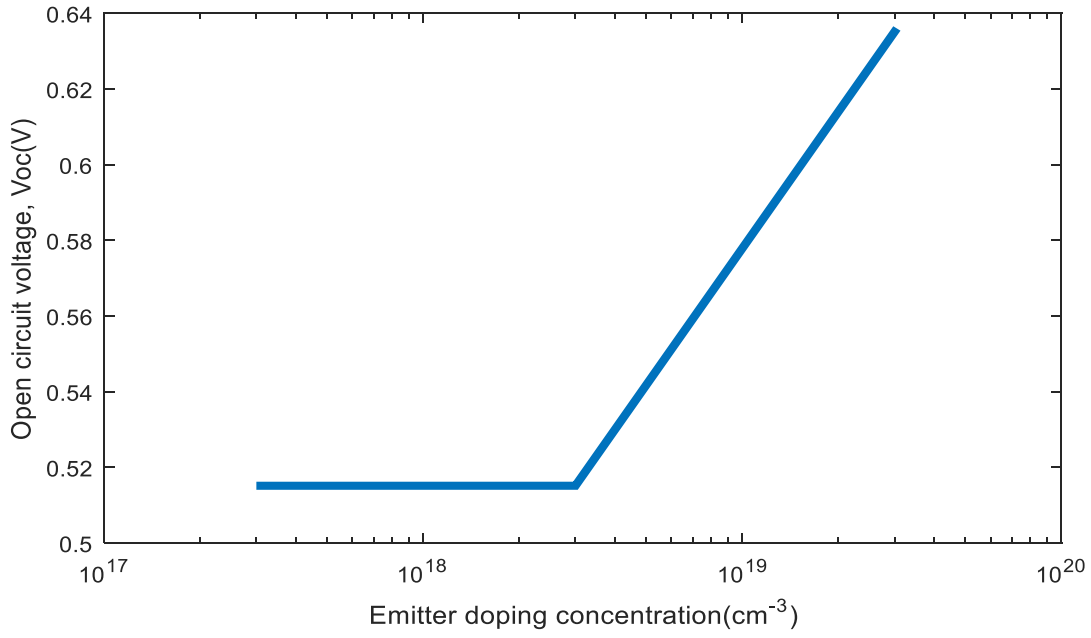

Figure 4.9: The open circuit voltage of HIT solar cell as a function of nc-Si:H p-layer concentration.

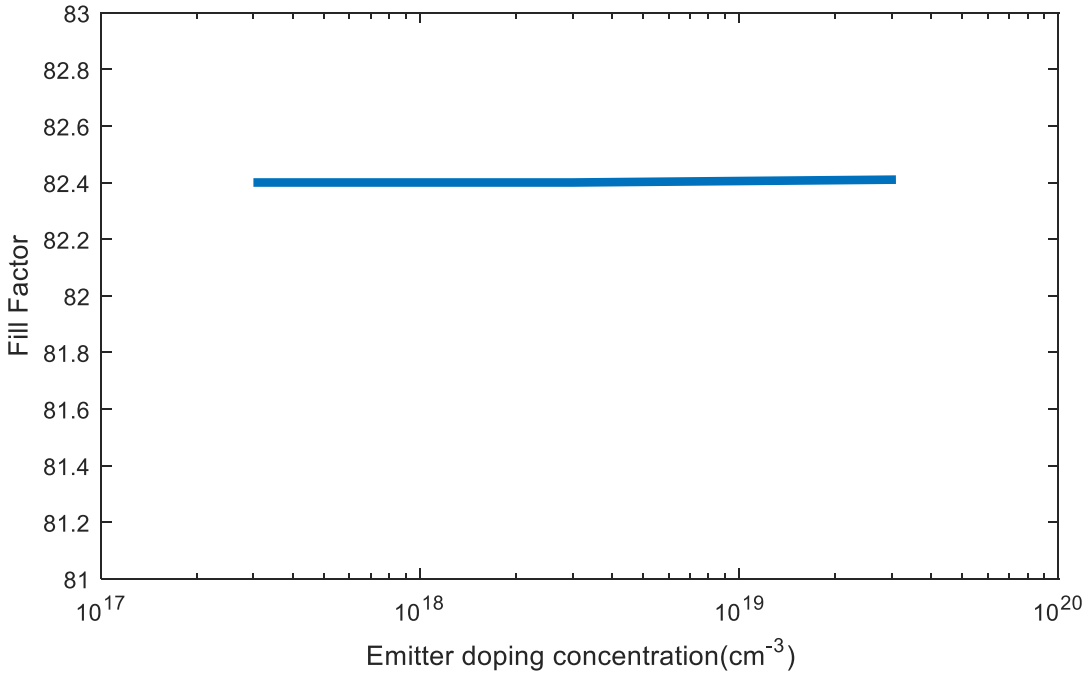

Figure 4.10: The fill factor of HIT solar cells as a function of the nc-Si:H (P^+) concentration.

At the front contact of the cell, the P^+ emitter concentration will be varied. When we increase concentration of the emitter then bend bending occurs. So that the holes will get more chance to tunnel through the interface of c-Si to nc-Si:H (p^+) and will get more absorption rate by the P^+.

With increasing the doping concentration of the nc-Si:H (p^+) emitter, the efficiency increases shown in figure 4.7. If a large doping concentration is adopted, the influence of defects states is weakened as well. We also observe that the open circuit voltage increases when the doping concentration changes from 3×10^{18} cm^{-3} to 3×10^{19} cm^{-3} shown in figure 4.9. But we observe that, the short circuit current and fill factor do not show any variation with increasing emitter doping concentration shown in figure 4.8 and figure 4.10.

4.3.1 Band bending trend due to concentration change of emitter

At the time of changing the concentration of nc-Si:H (P^+) emitter, we observe that the energy band diagram can explain the physics of changing characteristics. Here we witness that the more we increase the concentration of the emitter, the tunneling of the holes become easier from c-Si to nc-Si:H (P^+). The interface between c-Si (n) and nc-Si:H (P^+) blocks electron from c-Si (n) to nc-Si:H (P^+) at the conduction band but it allows hole from c-Si (n) to nc-Si:H (P^+) at valence band. From figure 4.11 to 4.13 with the increasing of emitter concentration, it is easier for holes to tunnel from c-Si (n) to nc-Si:H (P^+). We know that, generally hole wants to go to higher energy level. With increasing emitter doping concentration, the band bends more and holes get more opportunity to tunnel from c-Si (n) to nc-Si:H (P^+) because of the higher energy level of emitter side which are shown in figure 4.11 to 4.13.

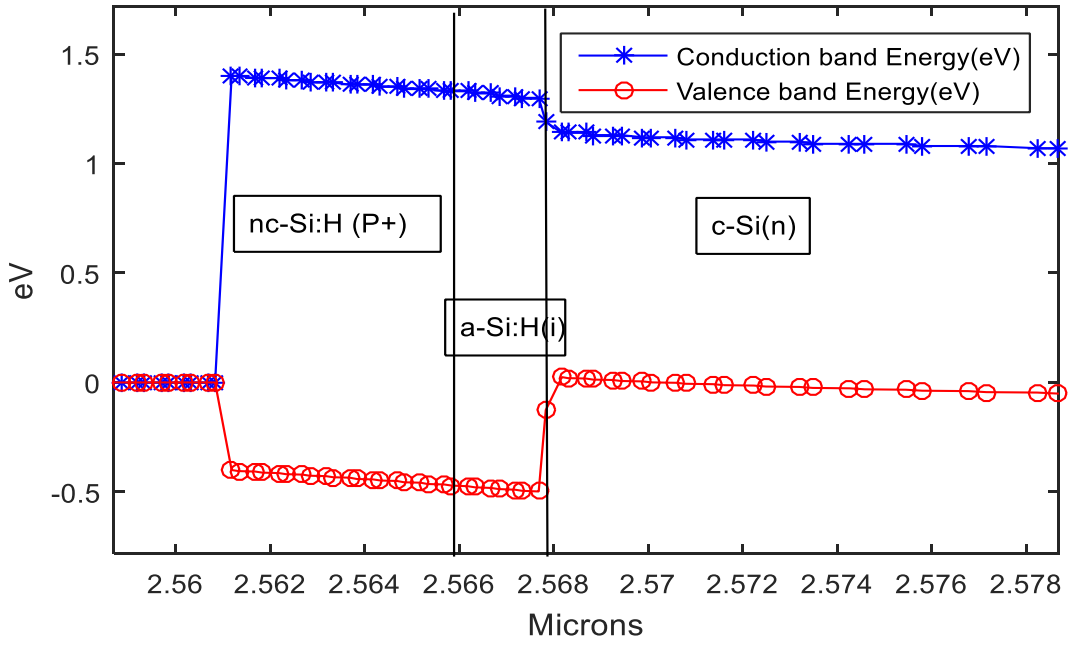

Figure 4.11: Band bending of HIT solar cell as a function of nc-Si:H (P^+) concentration when $3\times10^{17}cm^{-3}$.

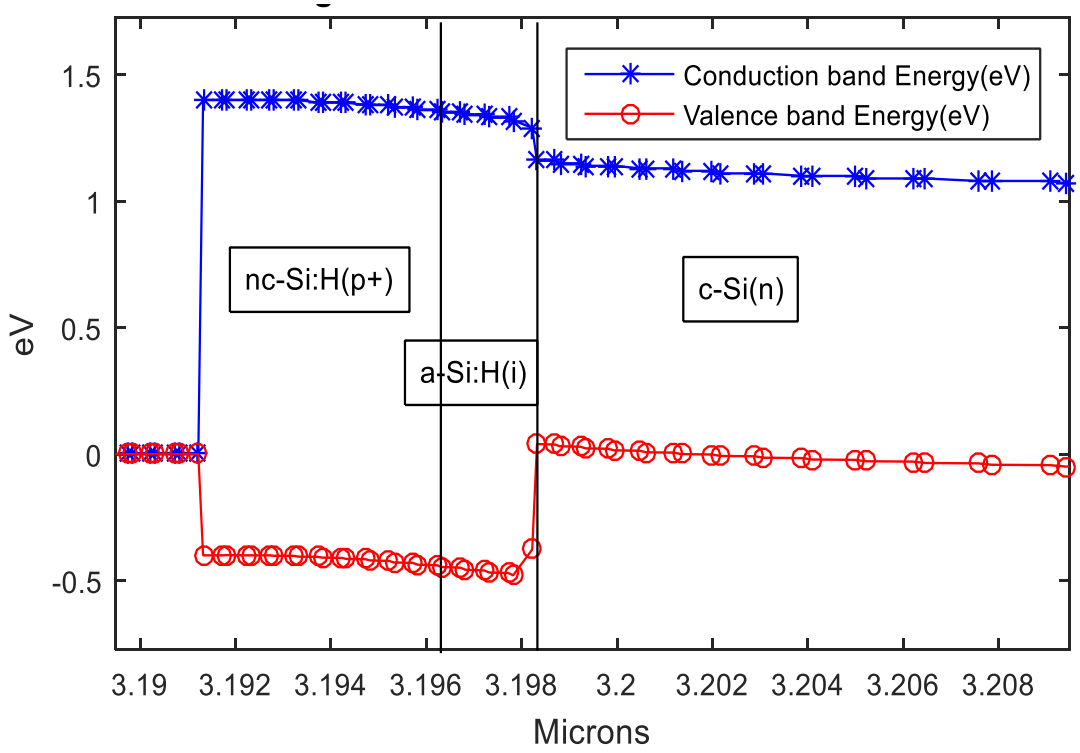

Figure 4.12: Band bending of HIT solar cell as a function of nc-Si:H (P^+) concentration when $3\times10^{18}cm^{-3}$.

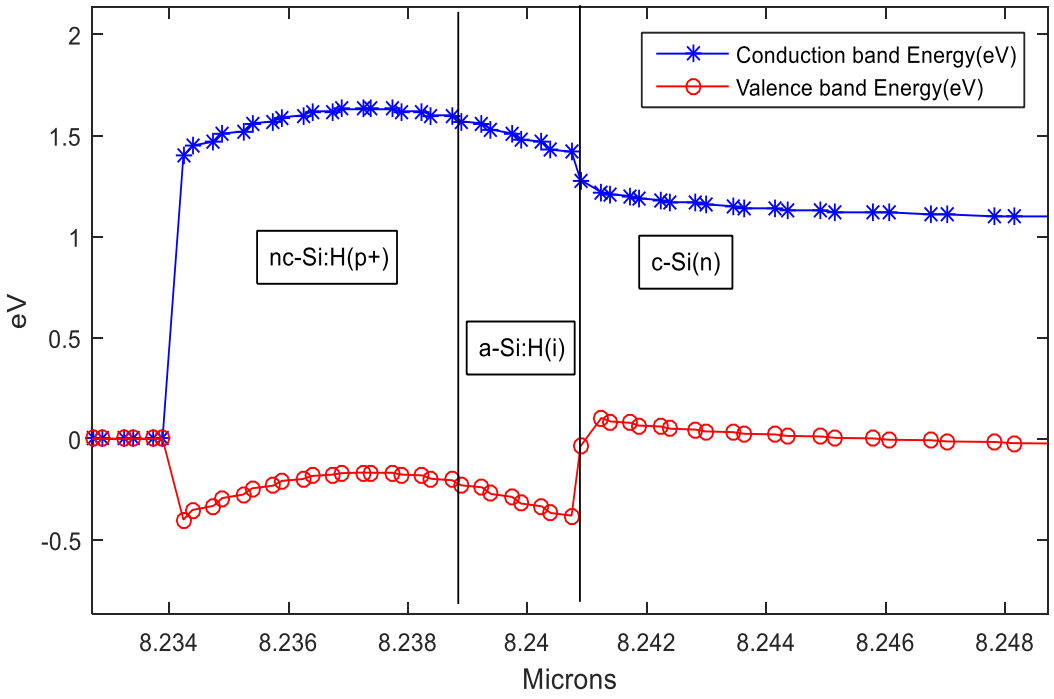

Figure 4.13: Band bending of HIT solar cell as a function of nc-Si:H (P^+) concentration when $3\times10^{19}cm^{-3}$.

4.4 Effect of the work function of the ITO layer

Work function of the conventional transparent conductive oxides, such as indium-tin-oxide (ITO), Zinc Oxide (ZnO) and so on, is usually high, generally in the range of 4.5-5.3 eV [7, 17]. With increasing work function of ITO, the efficiency of the HIT solar cell increases which is shown in figure 4.14. Besides, the energy band alignment creates an electric field at the interface ITO/nc-Si:H (p^+) which prevents the movement of holes from nc-Si:H (p^+) to ITO [18]. It is found that with increasing work function of ITO, the action of the electric field is weakened. Not only that, the built-in potential increases as well. Therefore the open circuit voltage and short circuit current increases shown in figure 4.15 and figure 4.16. The fill factor increases with increasing work function shown in figure 4.16.

The changes of the work function and thus the result of it on characteristics of the HIT solar cell are shown from figure 4.14 to 4.17. Here, the rest of the parameters of the HIT solar cell remain unchanged as followed the table 3.1.

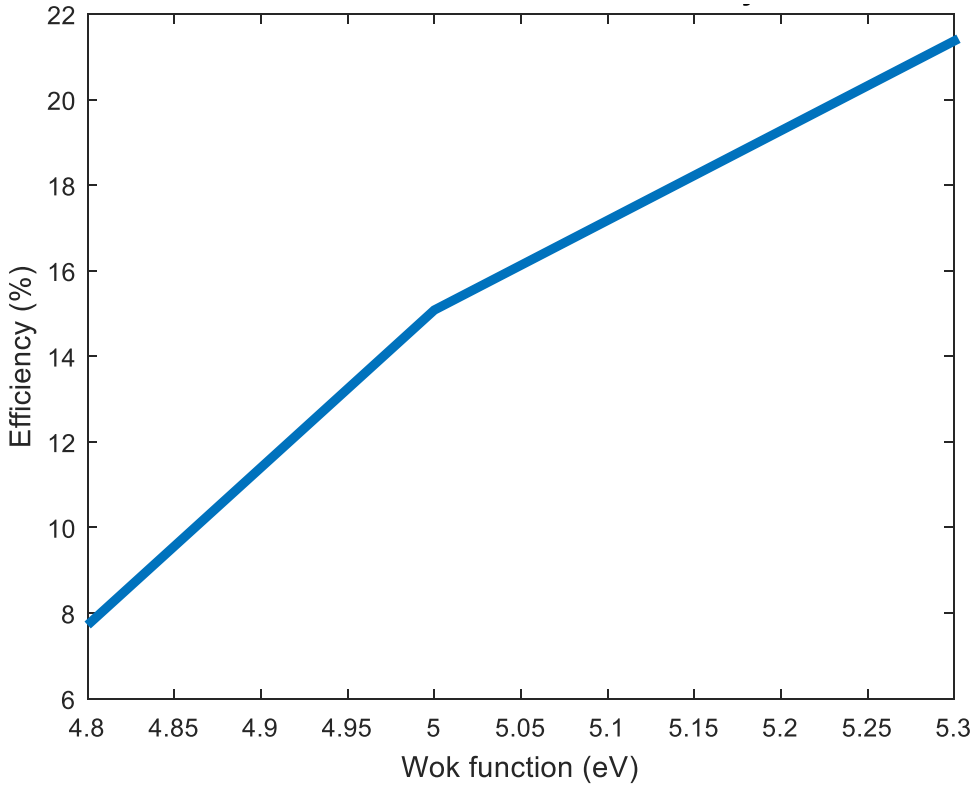

Figure 4.14: Work function of ITO effect on efficiency of HIT solar cell.

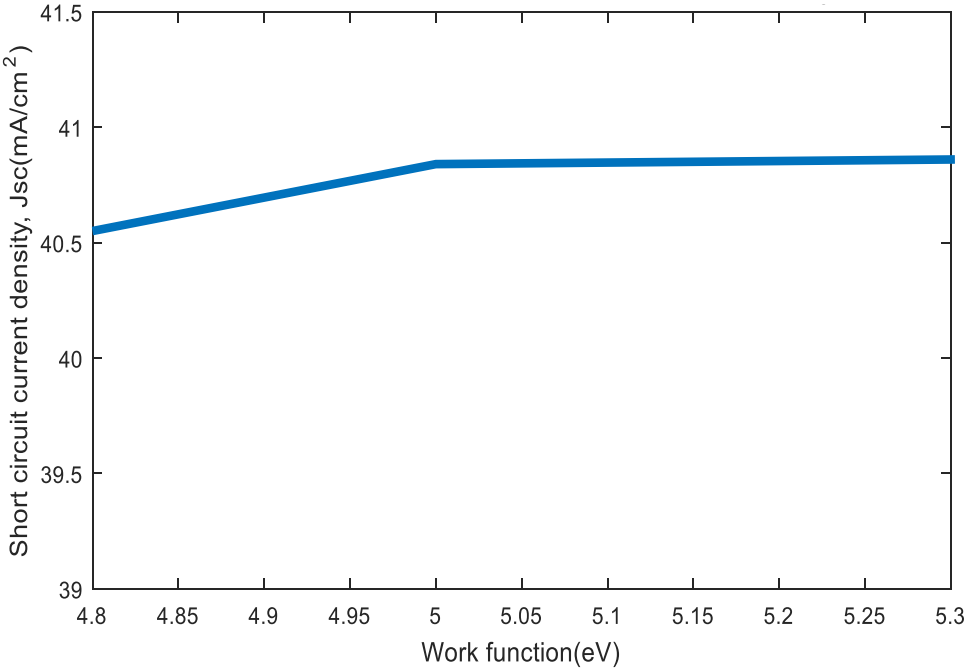

Figure 4.15: Work function of ITO effect on short circuit current of HIT solar cell.

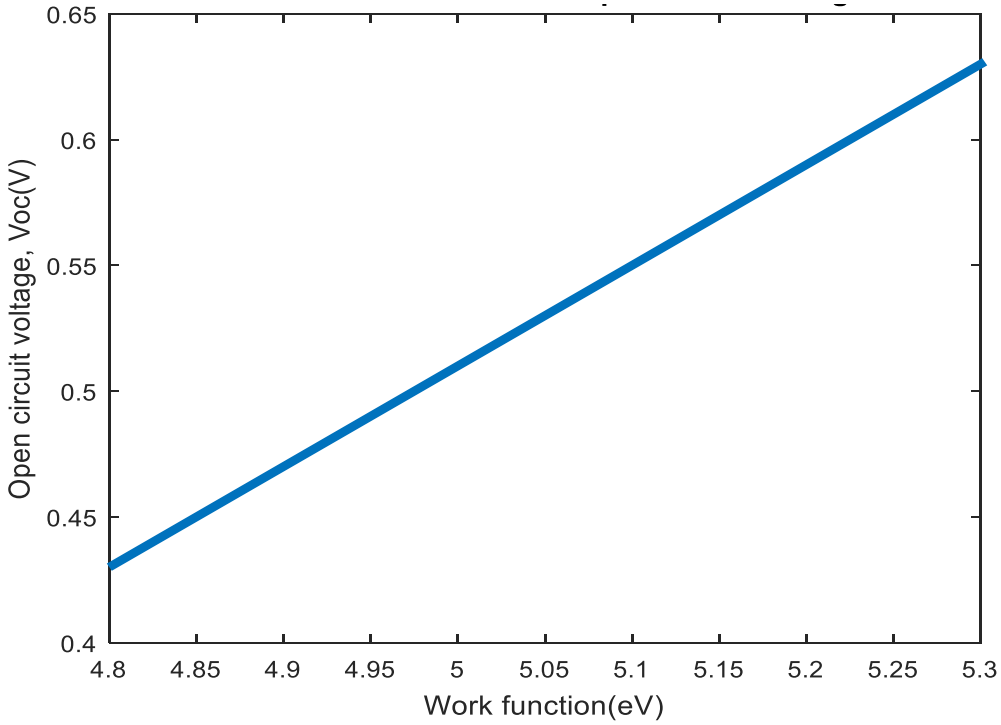

Figure 4.16: Work function of ITO effect on open circuit voltage of HIT solar cell.

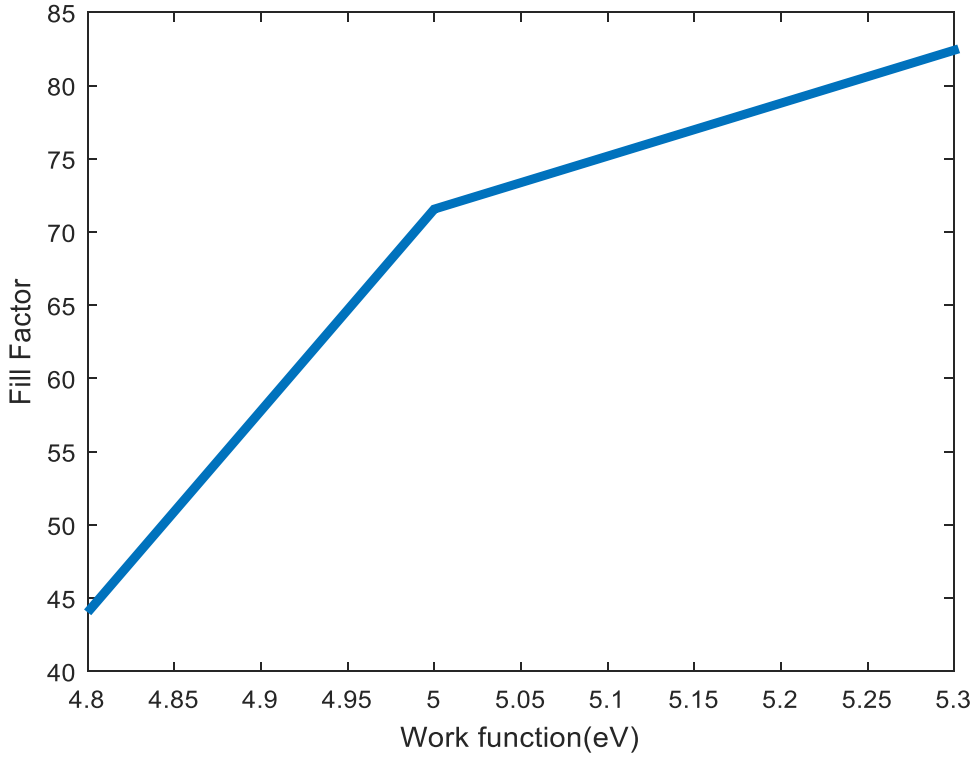

Figure 4.17: Work function of ITO effect on fill factor of HIT solar cell.

4.4.1 Band bending trend due to work function change of ITO layer

At the time of changing the work function of the front contact, we observe that the energy band diagram can explain the physics of changing characteristics. Here we observe that the more we increase the work function of the contact (Up to a defined level) the overall performance increases. When the work function is 4.8 eV the electric field between ITO and nc-Si:H (p^+) is comparatively bigger than the electric field when the work function is 5.0 eV. So that the holes will get collected in the contact more easily which is shown in figure 4.18 and figure 4.19. The electric field decreases more when the work function is taken 5.3 eV. Therefore, the collection of holes is increased shown in figure 4.20. As a result, the overall performance is increased due to increasing work function of front contact.

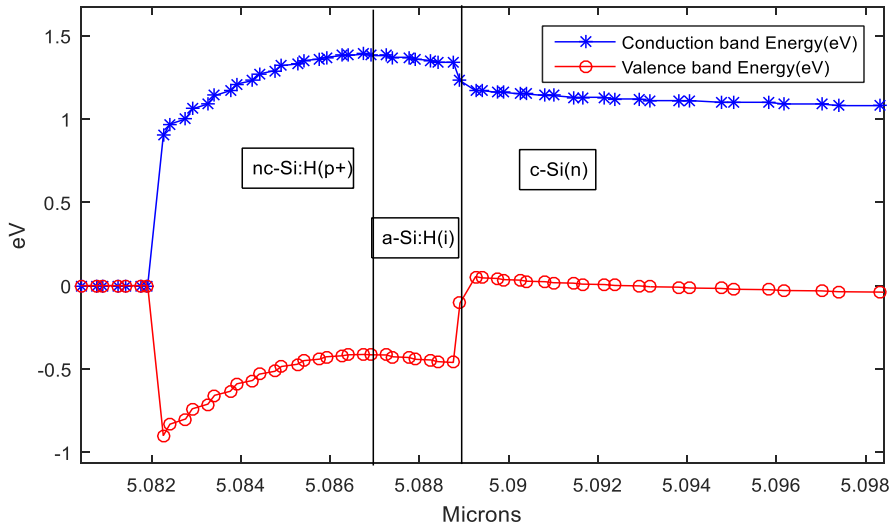

Figure 4.18: Band bending as a function of work function (4.8 eV) of ITO.

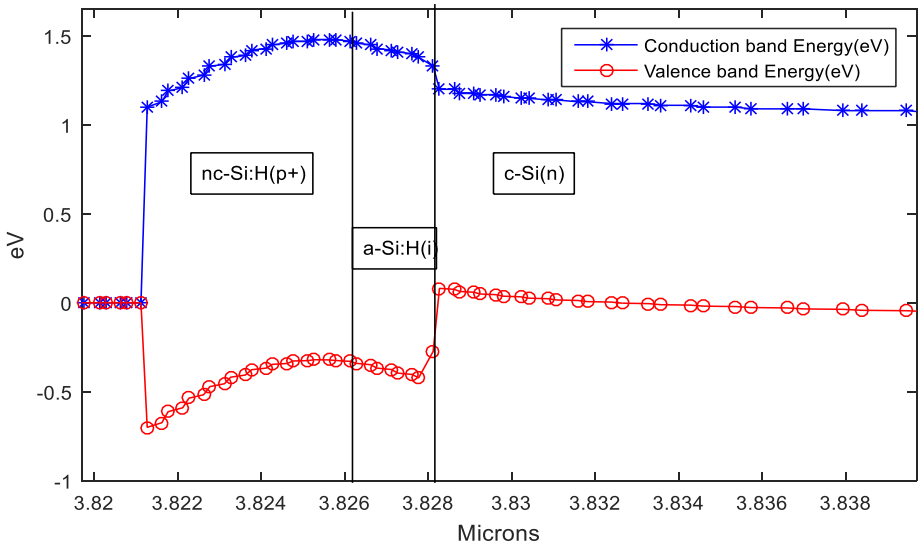

Figure 4.19: Band bending as a function of work function (5.0 eV) of ITO.

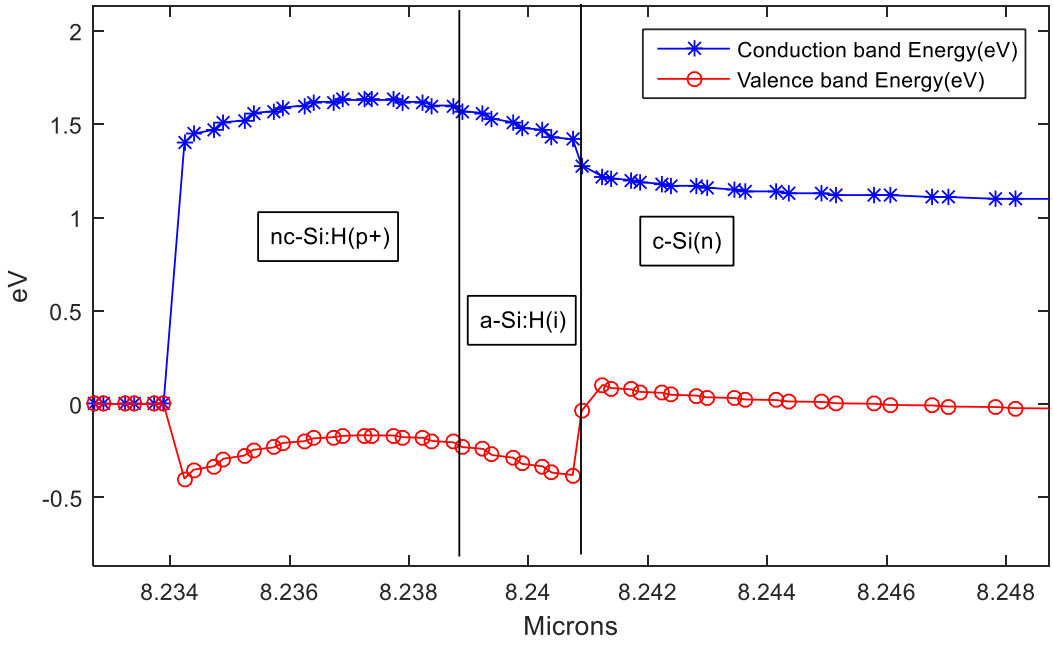

Figure 4.20: Band bending as a function of work function (5.3 eV) of ITO.

4.5 Effects of changing other parameters

Characteristics remain unchanged due to changing some parameter changes. When we change the length of the absorber c-Si, then the characteristics like efficiency, open circuit voltage, short circuit current and fill factor remain unchanged. This trend of unchanged behavior will be clear by observing in the table 4.1.

Table 4.1: Characteristics are remain unchanged due to the length of the c-Si absorber

C-Si (um)	Current(mA)	Voltage(V)	Fill factor	Efficiency (%)
100	40.7416	0.636705	82.5929	21.4249
300	40.7233	0.636526	82.4426	21.3703
500	40.7229	0.636555	82.2815	21.3293

Also the characteristics remain unchanged if the length of intrinsic a-Si layer of front side and back side are changes. There are no effects if the a-Si length changes.

Chapter 5: Conclusion

In this thesis, different parameters of HIT solar cell have been studied. This can be concluded as performance study of HIT solar cell. ATLAS SILVACO has been used to construct the structure and simulate these parameters. AMPS-1D is also used to simulate the results and for comparison purpose. The device has been simulated under standard spectrum AM1.5. Then open circuit voltage, short circuit current, efficiency and fill factor have been studied. Indium Tin Oxide (ITO) is used as TCO layer and front contact. Aluminum is used as back contact. The effects of changing different parameter values on HIT solar cell are mainly analyzed in this thesis work. The thickness of different regions and other material properties that are used for simulation are shown in table 3.1. The reasons of increasing or decreasing efficiency are discussed by showing energy band diagram. From the result, it is shown that the device has two sensitive parameters. The most sensitive parameter is the work function of ITO layer. If the work function of ITO layer can be increased, the efficiency can also be improved. Another sensitive parameter is the doping concentration of emitter. Efficiency increases with increasing emitter doping concentration. From the result of our thesis we observed that the material characteristics and the layer formation of the emitter, absorber and amorphous silicon are taken in a way so that we can get our desired result.

There are some possibilities of future work of HIT solar cell. The performance of the HIT solar cell can be improved by increasing the work function of transparent conductive oxide layer. We used ITO as transparent conductive oxide layer which has work function in the range of 4.5-5.3 eV. If the work function can be increased by using other materials then the overall performance can be improved. Defects states of the interface layer between the heterojunction of the cell can be improved further to increase the open circuit voltage.

References:

1. Photovoltaics report (2016). Fraunhofer Institute for Solar Energy Systems, ISE with support of PSE AG. Pg 24. Freiburg Germany.
2. T. Sawada et al., "High-Efficiency a-Si/c-Si Heterojunction Solar Cell," Conf. Record of the IEEE 1st World Conference on Photovoltaic Energy Conversion, Hawaii, USA, pp. 1219-1226, December 1994.
3. T. Mishima, M. Taguchi, H. Sakata, E. Maruyama, "Development status of high-efficiency HIT solar cells, Solar Energy Materials & Solar Cells," Solar Energy Materials and Solar Cells, vol. 95, issue 1, pp. 18-21, January 2011.
4. M. Taguchi, K. Kawamoto, S. Tsuge, T. Baba, H. Sakata, M. Morizane, K. Uchihashi, N. Nakamura, S. Kiyama and O. Oota, "HIT cells— high-efficiency crystalline Si cells with novel structure," Pro. Photovolt: Res. Appl., vol. 8, pp. 503-513, June 2000.
5. M. Taguchi, A. Terakawa, E. Maruyama, and M. Tanaka, "Obtaining a high V_{oc} in HIT cells," Pro. Photovolt: Res. Appl., vol.13, pp.481-488, February 2005.
6. C. Zhang, W Wei, "Model optimization of nanocrystalline Si:H HIT solar cells" Electric Information and Control Engineering (ICEICE), 2011 International Conference, Wuhan, China, pp. 1464-1468, 15-17 April 2011.
7. T. Minami, T. Miyata, T. Yamamoto, "Work function of transparent conducting multicomponent oxide thin films prepared by magnetron sputtering," Surf. Coat. Technol., vol. 108-109, pp. 583-587, October 1998.
8. M. Konuma, H. Curtins, F. A. Sarott and S. Veprek, "Dependence of electrical conductivity of nanocrystalline silicon on structural properties and the effect of substrate bias," Phil. Mag. B, vol. 55, pp. 377-389 March 1987.
9. S. Komuro, Y. Aoyagi, Y. Segawa, S. Namba, A. Masuyama, A. Matsuda, and K. Tanaka, "The dynamics of photoexcited carriers in microcrystalline silicon," J. Appl. Phys., vol. 56, pp.1658-1662, May 1984.
10. S. Ishihara, D. He, M. Nakata and I. Shimizu, "Preparation of High-Quality Microcrystalline Silicon from Fluorinated Precursors by a Layer-by-Layer Technique," Japan. J. Appl. Phys., vol. 32, pp. 1539-1545, January 1993.
11. K. Bhattacharya and D. Das, "Nanocrystalline silicon films prepared from silane plasma in RF-PECVD, using helium dilution without hydrogen: structural and optical characterization," Nanotechnology, vol. 18, pp. 415704-415712, August 2007.
12. M. A. Rifat and M. I. M. Khan, "Simulation study on the effects of changing band gap on solar cell parameters," Undergraduate Thesis, East West University, Dhaka, Bangladesh, p. 2, Spring 2016.
13. Makoto. T. (2010). Research and Development of Silicon Solar Cells in SANYO. Solar Energy Research Center SANYO Electric Co., Ltd.
14. M. Taguchi, et al. "An approach for the higher efficiency in the hit cells". Clean Energy Company, Sanyo Electric Co., Ltd. Pg 1.
15. N. Hernández Como, A. Morales Acevedo, "Simulation of heterojunction silicon solar cells with AMPS-1D," Solar Energy Materials & Solar Cells, vol. 94, pp. 62-67, May 2010.

16. Zhihua Hu, Xianbo Liao, Xiangbo Zeng, Yanyue Xu, Shibin Zhang, Hongwei Diao, Guanglin Kong, “Numerical simulation of nc-Si:H/c-Si heterojunction solar cells,” Acta Phys. Sin., vol. 52, pp. 217-224, January 2003.
17. J. S. Kim, B. Lägel, E. Moons, N. Johansson, I. Baikie, W. R. Salaneck, R. H. Friend, F. Cacialli, “Kelvin probe and ultraviolet photoemission measurements of indium tin oxide work function: acomparison,” Synth. Met., vol. 111–112, pp. 311-314, June 2000.
18. Yong Zhang, Yan Liu, Bin Lü, Hongying Zhang, Jiqing Wang, Naiyun Tang, “Influence of barrier height of the front contact on the amorphous silicon and microcrystalline silicon heterojunction solar cells, “ Acta Phys. Sin., vol. 58, pp. 2829-2835, April ,2009.
19. Antonio Luque, Steven Hegedus, Handbook of Photovoltaic Science and Engineering. John Wiley & Sons Ltd, 2002.